ESTIMATION OF MASS TRANSFER PARAMETERS IN A TAYLOR-COUETTE-POISEUILLE HETEROGENEOUS REACTOR

M. M. Resende[1], P. G. Vieira[1], R. Sousa Jr[1], R. L. C. Giordano[1] and R. C. Giordano[1*]

[1]Departamento de Engenharia Química, Universidade Federal de São Carlos,
Phone + (55) (16) 260-8264, Fax +(55) (16) 260-8266,
Via Washington Luiz km 235, C.P.676, 13565 905, São Carlos - SP, Brazil.
Email: roberto@deq.ufscar.br

Abstract - A bench-scale, continuous vortex flow reactor (VFR), with a radius ratio, η, equal to 0.48 and an aspect ratio, Γ, equal to 11.19 was studied. This reactor may be used in the enzymatic hydrolysis of polypeptides obtained from sweet cheese whey with enzymes immobilized on agarose gel. Operational conditions were $2410 < Re_\theta < 11793$ and 30-min residence time for glycerol-water, 14% w/w, 27°C (Re_{ax} = 1.1) and for water, 38°C (Re_{ax} = 1.5). Residence time distributions (RTDs) were obtained after pulse injections of different tracers (including dyed solid particles). Mass transfer coefficients of a lumped-parameter model of the reactor were estimated from these data. Model fitting to experimental data was accurate. Working conditions were selected so that transport properties of the fluids would be similar to the ones in the actual process at the final stages of whey hydrolysis.
Keywords: vortex flow reactor, hydrolysis, agarose, enzymatic reactor modeling, cheese whey proteolysis.

INTRODUCTION

Taylor flow is a secondary flow pattern that occurs in the gap between two concentric cylinders, an internal rotating one and an external, generally stationary, one. Above a critical rotation rate, accurately predicted by Taylor (1923), Couette circular flow becomes unstable and toroidal, alternate counterrotating vortices appear.

In Taylor-Couette-Poiseuille flow (TCP), an axial annular flux is added to the system and the apparatus may operate continuously. This flow regime has some features that are interesting for reaction and separation processes. The application of TCP to chemical reactors (vortex flow reactors, VFRs) was first developed by Kataoka (1975). The underlying idea was to take advantage of the relatively small interchange of mass between vortices (at least in the region of laminar flow) to enhance VFR performance. Linear theory predicts that the vortex drift velocity (ratio of the axial velocity of the vortex core to the superficial velocity), V_d, will be equal to 1.17 (Chandrasekhar, 1961). When V_d is equal to 1.0, all the vortices flow downward as a "stack", without any bypass or reflux stream and the system would approach a plug-flow pattern (Desmet et al., 1996).

Giordano et al. (1998) studied VFR behavior in the progressive vortex flow (PVF) region, where the toroidal, non-wavy vortices move downstream. Their work focused on small axial Reynolds numbers, Re_{ax} (0.172-1.067). It was observed that the vortex core slows its axial displacement for increasing rotations of the inner cylinder. V_d became zero for $Re_\theta / Re_{\theta,c}$

greater than 4.3. Campero and Vigil (1997) observed the same phenomenon in a two-liquid phase system. This may worsen the performance of the VFR, since the vortices become a pseudostagnant region when they stop displacement. However, this effect is partially counterbalanced by enhancing mass transfer to and from the vortex cores, when rotation rates of the inner cylinder increase. Hence, increasing Re_θ will transform the mixing characteristics of the VFR from an almost plug-flow to a perfectly mixed CSTR, but at intermediate rotations the reactor may show a CSTR-with-dead-volume behavior (Giordano et al., 2000a).

The present work studies the mixing characteristics of a heterogeneous VFR that contains suspended particles of agarose gel beads. These particles will be used as supports for immobilized proteolytic enzymes. The gentle but effective stirring caused by the vortices is adequate for working with fragile suspended particles. Examples of VFR applications are described in Kataoka et al. (1995), Sczechowski et al. (1995), Leitner et al. (1997), and Ameer et al. (1999).

This work presents residence time distributions (RTDs) for a reactor containing agarose gel spherical particles. Dyed particles and two solutes, methylene blue and blue dextran, were injected. Blue dextran does not diffuse into the particle pores, allowing detection of any effect of the solid phase on the mass transfer parameters fitted for the homogeneous reactor.

MATERIALS AND METHODS

The VFR jacketed vessel was made of acrylic and the inner (rotational) cylinder of polypropylene. A microcomputer, using an interface unit from T&S, São Carlos, controls the rotation with an accuracy of ± 1 rpm. Table 1 displays the VFR configuration.

Tracer could be injected at the reactor entrance, using a three-way valve, or at a side position. Strictly speaking, only the first option would generate RTDs, but both could provide useful information about mixing inside the VFR.

The mean residence time in the reactor was 30 min. With this value, a reasonable conversion would be achieved in the proteolysis. The critical rotational Reynolds numbers ($Re_{\theta c}$) for the onset of the Taylor instability were calculated in accordance with Recktenwald et al. (1993). Rates of rotation of the inner cylinder, necessary to sustain the agarose gel particles as a homogeneous suspension, were measured for each assay.

The load of particles in the VFR was 2% v/v in all cases, i.e., bed porosity was set at 98%. This is the catalytic load of the enzymatic reactor. A suspension of particles with the same load of solids (2% v/v) was continuously fed into the VFR (through a Masterflex peristaltic pump) during the experimental assays. Samples collected at the VFR exit were weighed, and it was observed that the 2% v/v ratio was sustained at steady state. At the end of each assay, the mass of particles inside the VFR was weighed to check the hypothesis of steady state.

RTDs were obtained after injection of pulses of blue dextran, Sigma, MW=2×10^6 Da and methylene blue, Vetec, MW=373 Da.

The tracer used to verify whether the particles might alter the mixing patterns of the liquid phase was blue dextran. This molecule does not diffuse into the pores and is not adsorbed on the gel matrix (Fernandez-Sanchez, 2000). In experiments without particles, RTDs using methylene blue were compared with the ones obtained with blue dextran to verify the influence of the molecular diffusivity of the tracer on the mass transfer parameters.

Table 1: VFR characteristics.

Dimensions (m)	Geometric characteristics
Inner cylinder radius........................1.25×10^{-2}	Radius ratio ($\eta = R_i/R_o$).................0.48
Outer cylinder inner wall radius.......2.60×10^{-2}	
Total height.....................................1.72×10^{-1}	Aspect ratio ($\Gamma = L/d$).....................11.2
Wetted region height.......................1.51×10^{-1}	

Tracer concentrations that guaranteed a linear response in the UV detector were 2×10^{-7} m^3 pulses of blue dextran 10 kg/m^3 (detection at 280nm) and 5×10^{-8} m^3 of methylene blue 5 kg/m^3 (665nm). In experiments with particles, samples were collected at the VFR exit and analyzed in UV spectrophotometer (Pharmacia Ultraspec 2000, 280 nm) after separating the gel beads by gravity. In blank experiments (without particles), the exit stream passed through UV continuous-flow cell (18 μl, Pharmacia). The holdup volume of the tubing at the reactor outlet was less than 0.1% of the VFR volume. Absorbance was continuously monitored with the Swift software from Pharmacia.

The particles were agarose gel 6 % w/w from Hispanagar, Spain with $\phi_{med.} = (55.0 \pm 9) \times 10^{-9}$ m^3. Their apparent density was 1.04×10^3 kg/m^3 (in water, 38ºC) and 1.11×10^3 kg/m^3 (in 14% w/w glycerol/water, 27ºC). Tracer particles had been previously dyed and injected with a syringe through the reactor inlet into the VFR loaded with colorless particles. After being collected, the samples were rediluted, and the fraction of dyed particles was assessed with an optical microscope; the experiments were always repeated trice. The tracer particles had an immobilized, deactivated enzyme (Penicillin G acilase) in their pores. Trypan blue (Sigma) adsorbs strongly on the immobilized enzyme, providing a deep blue coloration.

Two fluids were used: glycerol-water 14% w/w, T = 27 ºC (μ = 1.050×10^{-3} kg/m s and ρ = 1030 kg/m^3) and distilled water, 38ºC (μ = 0.760×10^{-3} kg/m s and ρ = 993 kg/m^3). These fluids had transport coefficients similar to those of cheese whey concentrate (with 52 kg/m^3 of protein) and to its hydrolyzed product at 50ºC, respectively. Cheese whey concentrate has μ = 1.050×10^{-3} kg/m s and ρ = 1027 kg/m^3. Hydrolyzed cheese whey (complete hydrolysis with trypsin and chymotrypsin) has μ = 0.774×10^{-3} kg/m s and ρ = 996 kg/m^3. All viscosities were measured in a Brookfield viscometer, model DV-III.

A Neslab thermostatic bath and a jacket controlled the temperature. An interface unit, T&S, São Carlos, connected to a PC was responsible for actuation and data acquisition. A continuous-current motor moved the VFR inner cylinder.

Mass transfer parameters were estimated using either a direct-search procedure or the Marquardt (1963) algorithm.

MATHEMATICAL MODELING

A more detailed description of the model, including the boundary conditions of the mass balance equations, may be found in Giordano et al. (2000b) and Resende et al. (2000). We will assume that vortex length does not change in the reactor, except for the three bottom and the three top vortices. The reactor is divided into stages and each stage consists of one vortex core and its neighboring bypass region. When the inner cylinder rotates at high speed, the vortices do not move with respect to a stationary frame (V_d = 0.0). This is the case for the experiments carried out here. The minimum rotation to guarantee a homogeneous suspension of particles was high enough to stop downstream displacement of the vortices.

The main hypotheses of the model are as follows:
1) The VFR is formed of stages consisting of a vortex core and its neighboring bypass region.
2) For each stage, the vortex core and the bypass stream are perfectly mixed regions with homogeneous (although different) concentrations.
3) The height of each stage is equal to the height of its corresponding vortex core (and is usually equal to the gap between cylinders).
4) The stages move downstream at a known velocity in relation to a fixed frame of reference; in all experiments reported on this work, this velocity is equal to zero (therefore, here V_d = 0.0 and the vortices are stationary).
5) The toroidal vortices have a circular cross section in the radial direction.
6) There is no "overlapping" of vortices; inflow and outflow boundaries separate different stages at horizontal planes.
7) Mass transfer between the vortex core and the bypass flow is governed by a coefficient, k.
8) Effects of axial dispersion in the bypass stream are lumped together in parameter Δ; a finite differences approach is applied and each stage is assumed to be an elementary volume.
9) Whenever a vortex contracts, mass transfer is unidirectional: the vortex loses mass to its vicinities (the surrounding bypass region); the opposite occurs when the vortex expands: it absorbs mass from the contiguous bypass region.

This model is generic. The situation described in item 9, however, did not occur for the assays presented in this work because the vortices were

stationary. The value of V_d must be known beforehand, but in our case, it was zero.

Mass balance equations, which constitute the model, are (for component j in the i stage):

$$V_i^e \frac{dC_{j,i}^e}{dt} = AU_{ax}(C_{j,i-1}^e - C_{j,i}^e) + (C_{j,i}^e - C_{j,i}^v/K_j)\frac{dV_i^v}{dt} +$$

$$+2\Delta_j.A\left[\frac{(C_{j,i+1}^e - C_{j,i}^e)}{(z_{i+1} - z_{i-1})} - \frac{(C_{j,i}^e - C_{j,,i-1}^e)}{(z_i - z_{i-2})}\right] - \qquad (1)$$

$$k_j S_i^v (C_{j,i}^e - C_{j,i}^v/K_j) + r_{j,i}^e V_i^e$$

$$V_i^v \frac{dC_{j,i}^v}{dt} = k_j S_i^v (C_{j,i}^e - C_{j,i}^v/K_j) + r_{j,i}^v V_i^v \qquad (2)$$

The reaction rates $r_{j,i}$ were zero during the RTD assays. Gel particles were treated as a pseudohomogeneous solute. For all solutes, the vortex-bypass partition coefficient K_j was equal to one. According to this model when $V_d = 0.0$, the net axial flow of fluid and particles would occur along the bypass stream and the vortices would be stagnant regions. Nevertheless, since Re_θ is high (to sustain the suspension of particles), the vortex-bypass mass transfer will be considerable. It should be stressed that equations (1) and (2) are valid for the particles as well.

RESULTS AND DISCUSSION

The operational region spanned by this work was $1.1 < Re_{ax} < 1.5$ and $2410 < Re_\theta < 11793$ (i.e., $1607 < Re_\theta / Re_{ax} < 7862$). In this region, the particles distribution was uniform and the vortices did not move downstream. Two tracers were used, blue dextran ($D_M = 1.058 \times 10^{-11}$ m^2/s, 25°C, in water) and methylene blue ($D_M = 1.663 \times 10^{-10}$ m^2/s, ibid). The difference between the response curves was insignificant. This is an indication that the influence of the solute diffusion coefficient can be neglected, as already observed by Moore and Cooney (1995).

Effect of the Presence of Particles

The RTDs presented in Figure 1 show the effect of the presence of suspended gel particles on the VFR response to pulses of blue dextran. It can be seen that the particles do not change the mixing characteristics of the reactor, at least for the high bed porosity that was used here (98%).
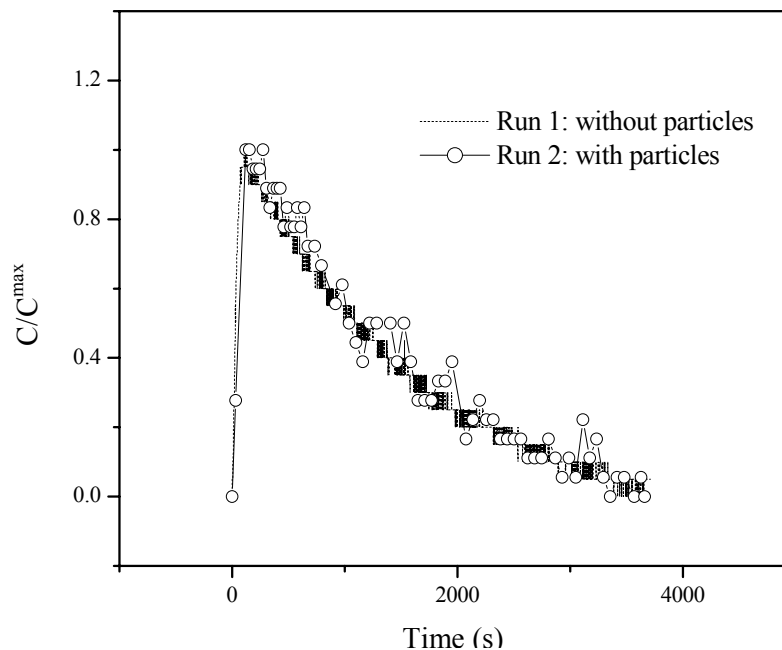

Figure 1: Influence of the suspended particles in the VFR. Tracer: blue dextran. Run 1: homogeneous reactor. Run 2: 2% v/v agarose gel (heterogeneous reactor). Working fluid: water 38°C; residence time: $\tau = 1800$ s; $Re_{ax} = 1.5$ ($U_{ax} = 8.37 \times 10^{-5}$ m/s); $Re_\theta = 11782$ ($\omega = 52.33$ s^{-1}).

Parameters

Increasing the rotation of the inner cylinder will enhance the axial dispersion parameter, Δ, and the vortex-bypass transfer coefficient, k. The reactor will ultimately approach a perfectly mixed CSTR. Correlations for the mass transfer parameters in dimensionless form, as a function of Re_θ, are presented in Equations (3) and (4). The range of Re_{ax} studied here (1.1-1.5) was narrow, and therefore the influence of axial flow on mass transfer could not be detected. Although this might be a limitation of the proposed correlations, it should be stressed that for our purposes, i.e., using the VFR for enzymatic reactions, equations (3) and (4) spanned the lower range of residence times and for higher values of τ the effect of Re_{ax} would certainly be even less important.

$$Pe_m = \frac{U_{ax}L}{\Delta} = 0.38\text{-}2.85\times10^{-5}\,Re_\theta \qquad (3)$$

$$k/\omega R_i = 3.48\times10^{-6}+1.98/Re_\theta$$

with

$$1.1<Re_{ax}<1.5 \text{ and } 2410<Re_\theta<11793 \qquad (4)$$

$$(1607<Re_\theta/Re_{ax}<7862).$$

Figure 2 shows the quality of the fit. The experimental point corresponding to the lower rotational Reynolds number was discarded because the suspension of particles was not homogeneous. They tended to settle to the bottom of the VFR and this fact was reflected in low values for the parameters k and Δ.

Figure 3 is a typical result, exemplifying the quality of the fitting when the Marquardt algorithm did converge. 95% confidence intervals of the parameters are reported, together with their correlation coefficient and co-variance matrix. The high uncertainty on the estimate of k should be pointed out. As it is usual for this kind of model, a large negative correlation is observed between k and Δ. A re-parameterization procedure, however, would not be possible in the frame of the present model structure. Since the fitting is very good, and the model has sound phenomenological basis, it was adopted despite of the high correlation between the parameters. Figure 3 also shows the DTR of a perfectly mixed CSTR, which consistently deviates from the experimental data.
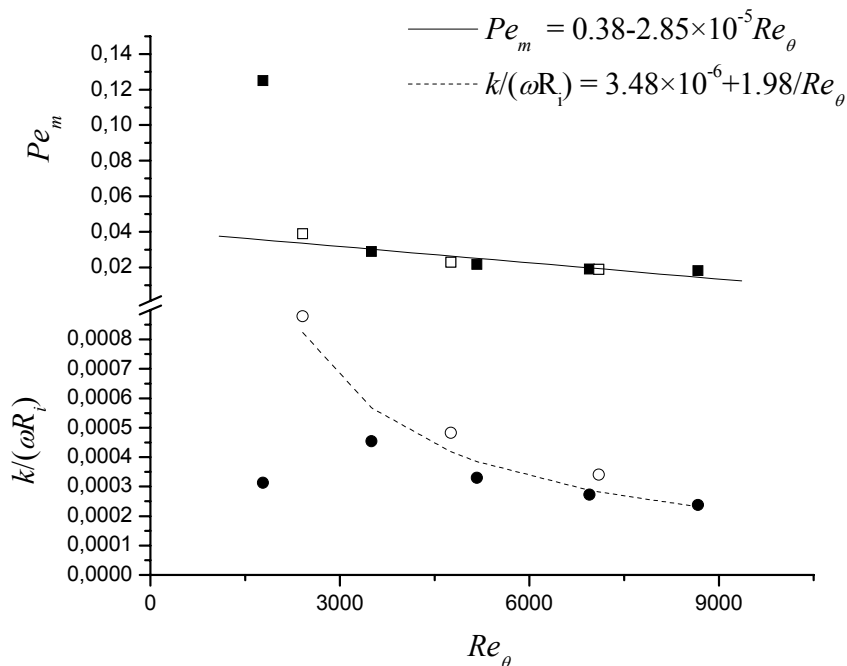

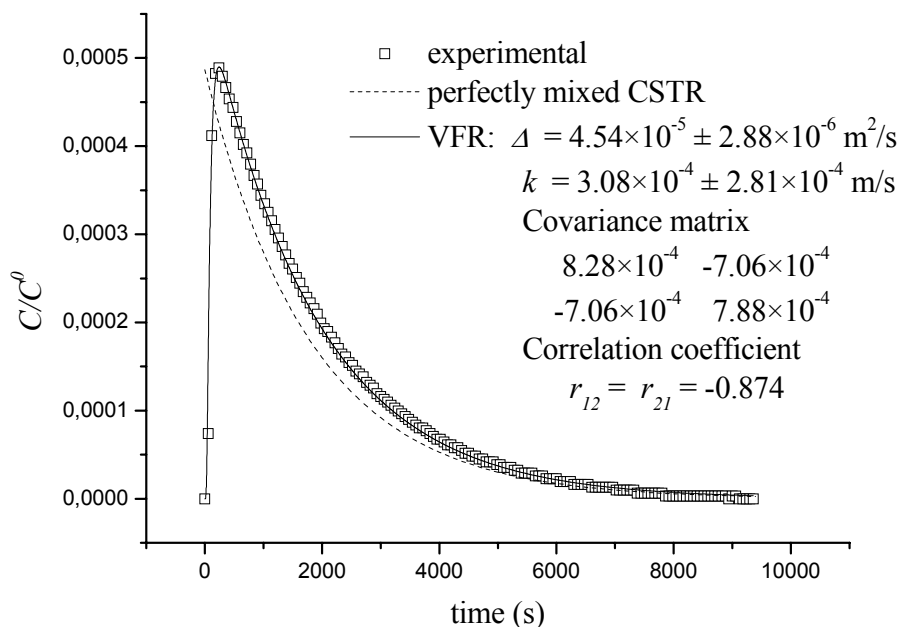**Figure 2:** VFR mass transfer parameters. Exp.: □, ○, water 38°C; ■, ●, glycerol 14% w/w and 27°C.

Figure 3: Experimental and simulated responses of the VFR to an injection of methylene blue at the reactor inlet. Working fluid: water 38ºC, $\tau = 1800$ s, $Re_{ax} = 1.5$ ($U_{ax} = 8.37 \times 10^{-5}$ cm/s); $Re_{\theta} = 4750$; ($\omega = 21.26$ s^{-1}).

Table 2 compares axial dispersion coefficients, estimated according to two different correlations (both based on the classic one-dimensional axial dispersion model), and our value for Δ under the same conditions. The parameters are on the same order of magnitude, and a good agreement is observed with the correlation of One question that arises is whether two parameters are actually necessary to model the VFR. Figure 4 shows the sensitivity of the two-parameter model with respect to k (vortex-bypass mass transfer coefficient), for two extreme values of Δ. The response of the axial dispersion model is also plotted. Results of the one-parameter model are biased (recalling that the fit of

the VFR model to the experimental data was excellent, as shown in Figure 3). The one-parameter model always predicts a higher degree of mixing in the reactor. The simulations using the VFR model, on the other hand, correctly indicate that decreasing the vortex-bypass parameter, k, would cause the RTD profile to reflect a more segregated flow pattern. Once again, the physical consistency of the model proposed here is observed. Therefore, it is reasonable to assert that the two-parameter model provides a sounder basis for simulating process situations when the reactions would take place.

Table 2: Axial dispersion coefficients. Operational conditions: Working fluid: water 38ºC; tracer: methylene blue ($D_M = 2.09 \times 10^{-10}$ m^2/s); residence time: $\tau = 1800$ s, $Re_{ax} = 1.5$ ($U_{ax} = 8.37 \times 10^{-5}$ m/s).

Reference	D_{ax} or Δ (m^2/s)
Levenspiel (1999), p. 310[*]	1) If d_t = d (gap) = 1.35×10^{-2} m $\Rightarrow D_{ax} = 3.18 \times 10^{-5}$ 2) If $d_t = 2\sqrt{R_o^2 - R_i^2} = 4.56 \times 10^{-2}$ m $\Rightarrow D_{ax} = 3.77 \times 10^{-4}$
Moore and Cooney (1995)	$D_{ax} = 4.58 \times 10^{-5}$
This work (for $Re_{\theta} = 3300$)	$\Delta = 4.54 \times 10^{-5}$

[*] This correlation is for cylindrical tubes. Since the VFR has an annular section, two different diameters, d_t, were used to estimate the axial dispersion: 1) assuming that the characteristic distance is the annular gap and 2) using an equivalent diameter, that would provide the same flow cross section.
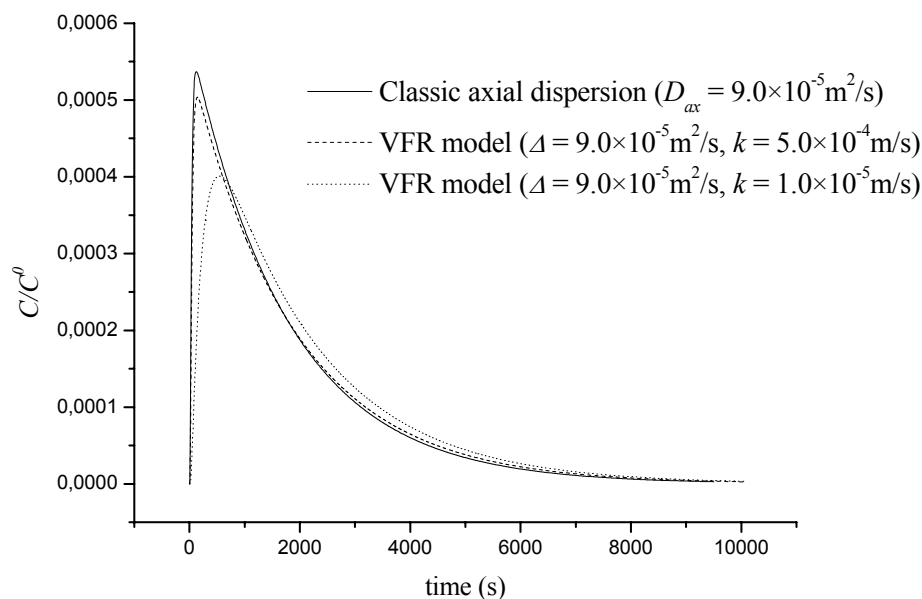
(a)
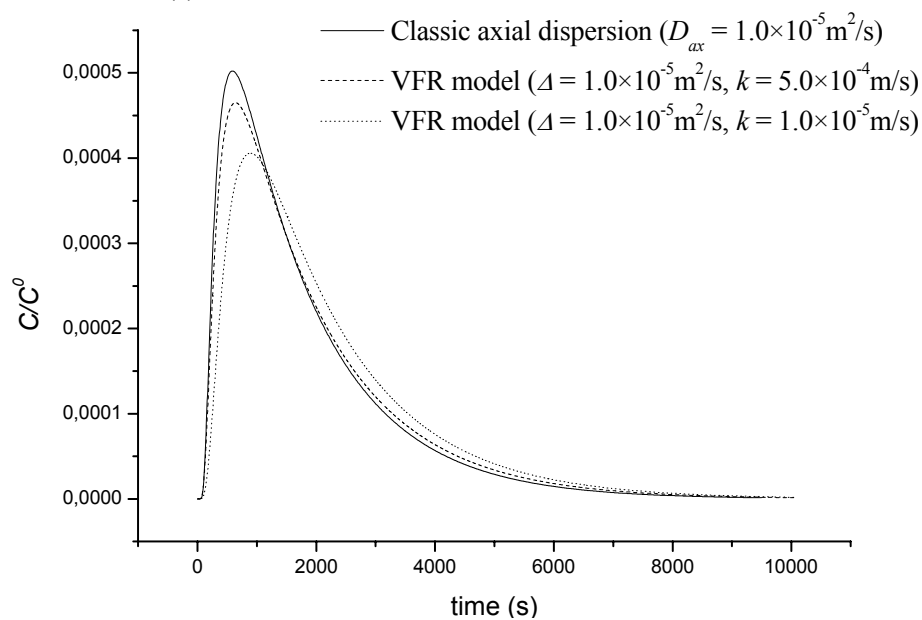
(b)

Figure 4 a, b: Parametric sensitivity of the VFR model with respect to the vortex-bypass mass transfer coefficient k, for $Re_{ax} = 1.5$ and two extreme values of Δ. The straight line is the response of the classic dispersion model.

RTD of Particles

Previously dyed particles of agarose gel, 6 % w/w, were injected with a syringe at the reactor inlet and samples were collected at the reactor outlet. Mass transfer parameters could be estimated thereon. Figure 5 is an example. As already pointed out, residence time distributions of the particles were indistinguishable from those obtained with soluble tracers, at least for the

accuracy that we could achieve using our methodology. Therefore, parameters k and Δ for the particles had the same values as those obtained from injections of blue dextran or methylene blue. The partition coefficient K was equal to one for the bead porosity studied (98%). This is an indirect indication, provided by the model, that the particles are suspended uniformly inside the reactor and evenly distributed throughout the vortex core and the bypass region.
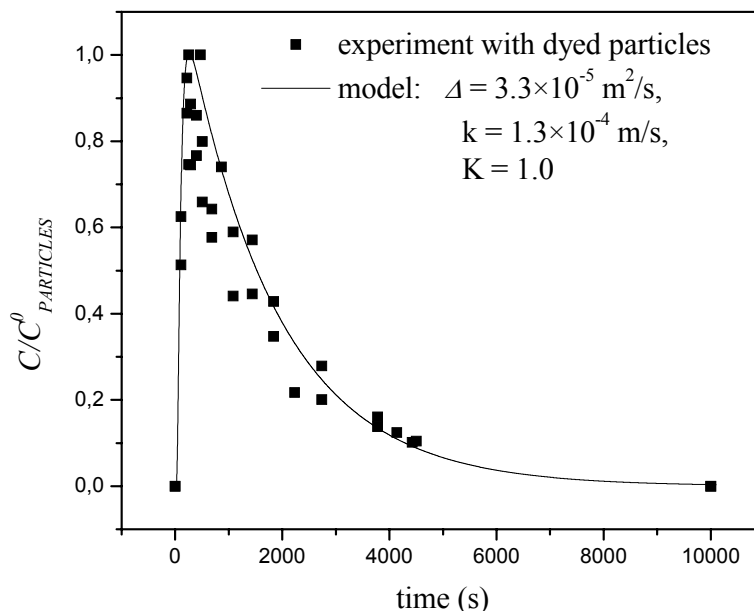
Figure 5: Experimental and simulated responses of the VFR to an injection of dyed particles at the reactor inlet. Bed porosity: 98%. Particles: 6% (w/w) spherical agarose gel. Working fluid: glycerol-water 14% w/w, 27 °C; $\tau = 1800$ s; $Re_{ax} = 1.5$ ($U_{ax} = 8.37 \times 10^{-5}$ m/s); $Re_\theta = 3500$ ($\omega = 21.26$ s^{-1}).

CONCLUSIONS

The values of the mass transfer parameters, k and Δ, calculated after fitting the model presented here to experimental residence time distributions, were consistent. For the operational range studied in this work, the proposed correlations were very accurate. Tracers of very different molecular sizes were tested (blue dextran and methylene blue) with similar results, which indicates that the molecular diffusion coefficient of the solute does not have an important influence on the mixing characteristics of the Taylor-Poiseuille flow. The injection of dyed agarose gel particles at the reactor inlet indicated that these particles behave as a pseudosolute, at least for the high bed porosity that was used here (98%). The particles had the same RTD as the tracers.

The correlations presented here can be used to model the enzymatic VFR, within the operational range appropriate for the proteolysis of cheese whey.

ACKNOWLEDGEMENTS

NOMENCLATURE

A	VFR annular cross section, m^2
C	VFR outlet concentration of tracer, kg/m^3
C^0	tracer mass/VFR volume (pulse injection), kg/m^3
C^{max}	maximum VFR outlet concentration of tracer, kg/m^3
C$^e_{j,i}$	concentration of component j in the bypass region of stage i, kg/m^3
C$^v_{j,i}$	concentration of component j inside vortex i, kg/m^3
d	annular gap width ($= R_o - R_i$), m
d$_t$	tube diameter in the correlation of Levenspiel (1999); see Table 2
D$_{ax}$	VFR axial dispersion coefficient, m^2/s
D$_M$	tracer molecular diffusion coefficient in water, m^2/s
k$_j$	vortex-bypass mass transfer coefficient of component j, m/s
K$_j$	vortex-bypass partition coefficient for the particles (C$^v_{j,i}$/ C$^e_{j,i}$), j = gel particle
L	axial length of the reactor, m
Pe$_m$	modified Peclet number ($= U_{ax} L/\Delta$)
Q	volumetric flow rate through the VFR, m^3/s
Re$_\theta$	rotational Reynolds number ($= \omega R_i d/\nu$)
Re$_{ax}$	axial Reynolds number ($= U_{ax} d/\nu$)

$r_{12} = r_{21}$ k-Δ correlation coefficient

$r^e_{j,i}$ rate of reaction of component j in the bypass region of vortex i, kg/m^{3}s

R_i inner (rotatory) cylinder radius, m

R_o outer (stationary) cylinder radius, m

$r^v_{j,i}$ rate of reaction of component j in vortex i, kg/m^{3}s

S^v_i external surface of toroidal vortex i, m^2

t   time, s

U_{ax} superficial velocity [Q/ A], m/s

V_d vortex drift velocity (speed of the vortex center/U_{ax})

V^e_i volume of the bypass region of stage i, m^3

V_i volume of stage i (= $V^e_i + V^v_i$), m^3

V^v_i volume of vortex core i, m^3

z_i axial coordinate of the upper boundary of stage i, m

Greek Letters

Γ aspect ratio (L/d)

Δ_j bypass axial dispersion coefficient of component j, m^2/s

η radius ratio (R_i/R_o)

ν kinematic viscosity, m^2/s

v_i fluid velocity relative to boundary i, m/s

ω angular velocity

ϖ_i velocity of the upper boundary of stage i with respect to a fixed frame, m/s

τ residence time

ν inner cylinder rotation rate, s^{-1}

REFERENCES

Ameer, G.A., Harmon, W., Sasisekharan, R. and Langer, R., Investigation of a Whole Blood Fluidized Bed Taylor-Couette Flow Device for Enzymatic Heparin Neutralization, Biotechnol. Bioeng., 62, p602-608 (1999).

Campero, R.J. and Vigil, R.D., Spatiotemporal Patterns in Liquid-Liquid Taylor-Couette-Poiseuille Flow. Phys. Rev. Letters 79, p3897-3900 (1997).

Chandrasekhar, S., Hydrodynamic and Hydromagnetic Stability, Clarendon Press, Oxford (1961).

Desmet, G., Verelst, H. and Baron, G.V., Local and Global Dispersion Effects in Couette-Taylor Flow – I: Description and Modeling of the Dispersion Effects, Chem. Engng. Sci., 51, p1287-1298 (1996).

Fernandez-Sanchez, V.M.F., Difusão de aminoácidos e proteínas em partículas de gel de agarose, Mater's thesys, Universidade Federal de São Carlos, Brazil (2000).

Giordano, R.C., Giordano, R.L.C., Prazeres, D.M.F. and Cooney, C.L., Analysis of a Taylor-Poiseuille Vortex Flow Reactor – I: Flow Patterns and Mass Transfer Characteristics, Chem. Eng. Sci., 53, p3635-3652 (1998).

Giordano, R.L.C., Giordano, R.C. and Cooney, C.L., Performance of a Continuous Taylor-Couette-Poiseuille Vortex Flow Reactor with Suspended Particles, Process Biochem., 35, p1093-1101 (2000a).

Giordano, R.L.C., Giordano, R.C., Prazeres, D.M.F. and Cooney, C.L., Analysis of a Taylor-Poiseuille Vortex Flow Reactor – II: Reactor Modeling and Performance Assessment Using Glucose-Fructose Isomerization as Test Reaction, Chem. Engng. Sci., 55, p3611-3626 (2000b).

Kataoka, K., Heat-Transfer in a Taylor Vortex Flow, J. Chem. Engng. Japan, 8, p271-276 (1975).

Kataoka, K., Ohmura, N., Kouzu, M. Simamura, Y. and Okubo, M., Emulsion Polymerization of Styrene in a Continuous Taylor Vortex Flow Reactor. Chem. Engng. Sci., 50, p1409-1416 (1995).

Leitner, N K.V., Le Bras, E., Foulcault, E. and Bousgarbiès, J.L., A New Photochemical Reactor Design for the Treatment of Absorbing Solutions, Wat. Sci. Tech., 35, p215-222 (1997).

Levenspiel, O., Chemical Reaction Engineering, 3rd ed., John Wiley, New York (1999).

Marquardt, D.W., An Algorithm for Least-Squares Estimation of Non-Linear Parameters, J. Soc. Ind. Appl. Math., 11, p431-441 (1963).

Moore, C.M.V. and Cooney, C.L., Axial Dispersion in Taylor-Couette Flow, A.I.Ch.E. J., 41, p723-727 (1995).

Recktenwald, A., Lücke, M. and Müller, H. W., Taylor Vortex Formation in Axial Through-Flow: Linear and Weakly Nonlinear Analysis, Phys. Rev. E, 48, p4444-4454 (1993).

Resende, M.M, Ferreira, A.L.S., Giordano, R.L.C, Giordano, R.C., Mass Transfer and Fluid Dynamics Study of a Taylor-Poiseuille Vortex Flow Reactor, Anais do XIII Congresso Brasileiro de Engenharia Química, COBEQ,

Águas de São Pedro-SP (2000).

Sczechowski, J. G., Koval, C. A. and Noble, R. D., A Taylor Vortex Reactor for Heterogeneous Photocatalysis, Chem. Engng. Sci., 50, p3163-3173 (1995).

Taylor, G. I., Stability of a Viscous Liquid Contained Between Two Rotating Cylinders, Phil. Trans. R. Soc. A, 223, p289-343 (1923).